Effect of Crack and Cutout on Vibration Characteristics of A Laminated Composite Plates Using Nonlinear Finite Element Analysis

Dr. Nabil Hassan Hadi *& Kayser Aziz Ameen

Received on: 1/3/2011
Accepted on: 21/7/2011

Abstract

A nonlinear finite element model for geometrically large amplitude free vibration analysis of composite laminated plate using high order shear deformation theory used in this work. The aim of the study is to analyze the effect of the stationary crack and hole on the free vibration of composite plate those in which the singularity due to presences of crack is modeled, so that stress field at the tip of the crack is properly represented. The results are computed for different crack, hole size, material orthotropy and different boundary condition. Finally the discrepancy of the results was 29.8249% when considered the severe nonlinearity.

Keywords : singularity crack, Hole, High order shear deformation, Plate, Free vibration, Nonlinear finite element Method.

تاثير الثقوب والشقوق على الخواص الاهتزازية للصفائح المركبة المتعددة باستعمال طريقة العناصر المحددة اللاخطية

الخلاصة

استعمل في هذا البحث طريقة العناصر المحددة اللاخطية للاشكال الهندسية وذات الذبذبات العالية للترددات الحرة وباستعمال نظرية القص العالية الرتبة. وان هدف هذه الدراسة هو تحليل تاثيرات الشقوق الساكنة والثقوب على الترددات الطبيعية للصفائح المركبة المتعددة الطبقات وتم اخذ النموذج الانفرادي للتحليل الشقوق حيث يكون قيم الاجهادات عند طرفي الشقوق مستوية لللانهاية. وتم دراسة تاثير حجم الثقوب والشقوق والخاصية التعامدية للمواد المركبة وكذلك الشروط الحدية على الترددات الطبيعية وان التناقض في النتائج عند الاخذ بنظر الاعتبار الحدود اللاخطية كان 29,8249%.

* Engineering College ,University of Baghdad/ Baghdad

https://doi.org/10.30684/ etj.29.12.9
University of Technology-Iraq, Baghdad, Iraq/2412-0758

Notations

α, β, ζ : Rectangular coordinate axes

$\bar{u}, \bar{v}, \bar{w}$: Displacement along the α, β, ζ coordinate

$\{\varepsilon_L\}, \{\varepsilon_{NL}\}$: Linear and nonlinear strain vectors

$[Q]$: Transferred reduced elastic constant

E : Young's modulus (GPa)

G : Shear modulus (GPa)

υ : Poisson's ratio

W_{max}/h : Amplitude ratio

ω_{NL}/ω_L : Frequency ratio

κ_{dL}, κ_{dNL} : Damage ratio for linear and nonlinear respectively $(\omega_{intact} - \omega_{delamenation})/\omega_{intact})$

Introduction

Cracks are one of the most common types of defects. A crack is a long narrow opening through material. The crack have sharp tips is considered the modeling of finite element methods for this case focused on the singularity point where quantities such as stress become (mathematically, but not physically) infinite.

All type of damages in composite structure result in change in stiffness, strength and fatigue properties. Measurement of strength or fatigue properties during damage development is not feasible because destructive testing is required. However, stiffness reduction due to damage can be measured since damage directly affects structural response, which provides a promising method for identifying the occurrence, location and extent of the damage from measured structural dynamics characteristics. Existence of cracks and cutout causes reduction in natural frequencies.

Adams et al.[1] found that, with fiber-reinforced plastics, a state of damage could be detected by a reduction in stiffness and an increase in damping, whether this damage was localized, as in a crack, or distributed through the bulk of the specimen as many micro cracks. This change in stiffness resulted in a change in the natural frequencies of the specimen. **Cawley and Adams**[2]**.** Developed a method of sensitivity analysis to deduce the location of damage based on the application of finite element method. The method was applied to a flat isotropic plate. The sensitivity of the change in eigenvalue was evaluated for each of the element in the model. A three dimensional finite element computer program has been developed by **James D. Lee**[3] to analyze layered fiber reinforced composite laminate. This program is capable of : (1) calculating the detailed stress distribution, (2) identifying the damage zone and mode of failure, (3) analyzing the damage accumulation, and (4) determining the ultimate strength of the composite laminate. A non linear laminate layer wise beam theory is developed to simulate the effect of interlayer slip. It shown that by definition of an effective cross sectional rotational, the complex problem reduce to simpler case of a homogeneous shear deformable beam with effective stiffness and corresponding set of boundary condition. This vibration analysis carried out for layered beam by **Adam C. and Ziegler F.1999** .**Yi Liu, Feng Jin and Qing Li**[4], presented a newly developed Fixed Grid evolutionary Structural optimization method to explore shape optimization of multiple cutouts in composite structures.

* Engineering College ,University of Baghdad/ Baghdad

Different design cases with varying number of cutouts, ply orientations and lay-up configuration are taken into account, also provides an in-depth observation in the interactive influence of the adjacent cutouts on the optimal shapes. **A. V. Singh and U. K. Paul**[5] studied by energy method for linear and geometrically nonlinear static analysis of thin isotropic plate with and with out cutout. The plates are subjected to uniformly distributed load and both the pinned and fixed outside boundary conditions are considered and the effects of the opening size on the displacement are examined in detail. **Cengiz Polat & Zülfü Çinar ulucan**[6], developed a geometrically nonlinear formulation for the axisymmetric plate and shell structures. The formulation is based on the total Lagrangian approach and are solved using the Newton Raphson method. In this paper study the effect of hole and crack on the natural frequency with different boundary condition, material orthotropy, hole size and crack size and mode shap when considered the severe nonlinearity.

Fadhel Abbas Abdulla[10],

study the effect of internal flaws (voids) in composite plate, using three type of solution (analytical, numerical and experimental solution). This work is investigated theoretically by using finite element method the effect of crack and hole on the natural frequency of the composite material with considering the severe nonlinearity, which is studied the modal analysis of intact and delamination plate.

Mathematical Model

Displacement field

A plate of length a, width b and thickness h is composed of N number of orthotropic layers of uniform thickness. The (α, β, ζ) was rectangular coordinate. The following displacement field for the laminated plate based on the high shear deformation theory (HSDT) is considered to derive the mathematical model. the displacement along the (α, β, ζ) coordinates.

$$\left.\begin{aligned}\bar{u}(\alpha,\beta,\zeta,t) &= u + \zeta\phi_1 + \zeta^2\psi_1 + \zeta^3\theta_1 \\ \bar{v}(\alpha,\beta,\zeta,t) &= v + \zeta\phi_2 + \zeta^2\psi_2 + \zeta^3\theta_2 \\ \bar{w}(\alpha,\beta,t) &= w\end{aligned}\right\} \quad (1)$$

Where t is the time, (*u,v,w*) are the displacements of a point on the mid-plane and ϕ_1 and ϕ_2 are the rotations at ($\zeta = 0$) of normal to the mid-plane respect to the α and β-axes, respectively, $\psi_1, \psi_2, \theta_1, \theta_2$ are high order terms of Tayler series expansion defined at the mid-plane (Panda and Singh, 2009).

Strain –displacement relation

The nonlinear Green Lagrange stain displacement relation for the laminated plate can be expressed as follows (Panda and Singh, 2009).

Substituting equation (1) into equation (2) in Appendix (A), the strain – displacement relation of the laminated plate is expressed as shown in Appendix (A) equation (3).

The value of individual terms of above equation which are provided in reference [Nabil Hassan Hadi and Kayser Aziz Ameen].Hence the above equation can be rearrangement as shown in Appendix (A) equation (4).

Stress - strain relations

In the analysis of composite laminated materials, the assumption of plane stress is usually used for each layer. This mainly because fiber reinforced material are utilized in beam, plate, cylinders, spherical and other structural shapes which have at least one characteristic geometric dimension in an order of magnitude less than the other two dimensions. In this case the stress components ($\sigma_3, \tau_{23}, \tau_{13}$)are set to zero. Then the strain displacement relations, for any general kth orthotropic composite lamina with an arbitrary fiber orientation angle with reference to the coordinate axes (α, β, ζ) is written as shown in equation (5) in Appendix (A).

Strain energy of the laminate

Energy and variational principle offered great simplification to many derivations of fundamental equations in elasticity. Also have been used to introduce and implement approximation techniques for structural systems. Strain energy is defined as the work done by the internal stresses which caused elongation or shear strains. The strain energy of the plate can be expressed as :

$$U = \frac{1}{2}\int_V \{\varepsilon\}_i^T \cdot \{\sigma_i\} dV \quad (6)$$

By substituting the strains from equation (2) and stresses from equation (5) into equation (6) the strain energy can be expressed as shown in equation (7) in Appendix (A).

Kinetic energy of the vibrating plate

The kinetic energy expression of a vibrated plate can be expressed as

$$T = \frac{1}{2}\int_V \rho \{\dot{\bar{\delta}}\}^T \{\dot{\bar{\delta}}\} dV \quad (8)$$

Where, ρ and $\dot{\bar{\delta}}$ are the density, displacement vector which differentia the first order of displacement with respect to time, respectively. The global displacement vector can be expressed as shown in equation (9) in Appendix (A).

Then the kinetic energy for 'N' number of orthotropic layered composite plate obtained by substituting the equation (9) into equation (8).

$$T = \frac{1}{2}\int_A \left(\sum_{k=1}^{N} \int_{\zeta_{k-1}}^{\zeta_k} \{\dot{\delta}\}^T [f]^T \rho^k [f] \{\dot{\delta}\} \mathrm{d}\zeta \right) \mathrm{dA}$$

$$T = \frac{1}{2}\int_A \{\dot{\delta}\}^T [m] \{\dot{\delta}\} \mathrm{dA} \quad \text{.....(10)}$$

Where, $[m] = \sum_{k=1}^{N} \int_{\zeta_{k-1}}^{\zeta_k} \left([f]^T \rho^k [f]\right) \mathrm{d}\zeta$

is the inertia matrix.

Solution Technique

The displacement vector can be conceded to the form by employing the FEM

$$\{\delta\} = [N_i]\{\delta_i\} \quad (11)$$

Where :

$$\{\delta_i\} = [u_i \quad v_i \quad w_i \quad \phi_1 \quad \phi_2 \quad \psi_1 \quad \psi_2 \quad \theta_1 \quad \theta_2]^T$$

The equations of strain for linear and nonlinear are studied of large deflections, as in equation (4) and nonlinear displacement in equation (1), when substituted into equation (7), the strain energy can be written as shown in equation (12).

The final form of governing equation for the nonlinear free vibration laminated plate panel is obtained by using Hamilton's principle. It can be viewed and axiom, from which other axioms like Newton's second law, Let us define the potential energy to be ($\Pi = U - W$), which U is the strain energy and W is the work done and the Lagrangian as the function L where *(L = (T – U+W))*.

Hamilton's principle states that the actual displacement that the body actually goes through from instant (t_1) to instant (t_2) out of many possible

paths, is that which achieves an extremum of the line integral
of the Lagrangian function. This is achieved if the variation of the time integral of the Lagrangian is set to zero:

$$\delta\int_{t_1}^{t_2} L\,dt = 0 \qquad (13)$$

Hamilton's principle can be used to find the compatible set of equations of motion and boundary conditions for given stresses and strains. This is done by substituting the equations for strain energy equation (12) and kinetic energy equation (10) into the equation (13), performing the integration by parts, and setting the coefficients of the displacement variations (also called virtual displacement) equal to zero. The Lagrangian becomes:-

$$[M]\{\ddot{\delta}\}+([K_L]+[K_{NL}])\{\delta\}=0 \quad (14)$$

Where $\{\delta\}$ is the displacement vector, *[M]*, *[K_L]* and *[K_{NL}]* are the global mass matrix and global linear stiffness matrix and nonlinear stiffness matrix that depend on the displacement vector respectively.

Damage modeling

Defect and damages cause the laminates to lose their strength and rigidity and also the safe working life is reduced. Defects and damages can creep in at any time like manufacturing, in service or in design due to discontinuities such as cut out and play drops. The investigation of defects and damages are presented. By using the following expansion of the displacements through the thickness of the plate.

Cracks are one of the most common types of defects. A crack is a long narrow opening through material. We consider the crack to have sharp tips. The modeling of finite element methods for this case focused on the singularity point where quantities such as stress become (mathematically, but not physically) infinite. Where the stress given by the equation bellow :

$$\{\sigma\}=[D][B]\{\delta\} \quad (15)$$

In the equation (15), if the stresses are to be singular, the [B] has to be singular. Consequently, if [B] is to be singular then the determinate of [J] must vanish to zero then the ($\frac{\partial x}{\partial \zeta}$ and $\frac{\partial y}{\partial \eta}$ must force to be zero). Considering a rectangular element of length L along as shown in the figure (1).

It can be seen the both off diagonal terms ($\frac{\partial x}{\partial \zeta}$ and $\frac{\partial y}{\partial \eta}$) are zero, making the proper substitution for $\frac{\partial x}{\partial \zeta}$ at $\eta=-1$, it has equation (16).

After simplification equation (16), and considering the first corner node (where $\xi=\eta=-1$), it can be get :

$$\frac{\partial x}{\partial \xi}=0 \Leftrightarrow x_5=\frac{L}{4}$$

Thus all the terms in the jacobian vanish if and only if the second node is located at ($\frac{L}{4}$) instead of $\frac{L}{2}$ and subsequently both the stresses and strains at the first node will become singular as shown in figure (2).

As shown in the above figure that the stresses at the first node are singular, to find the degree of singularity. First let us solve for ξ in terms of x and L at ($\eta = -1$) (that is a long side 1-5-2):

$$x = \sum_{i=1}^{8} N_i x_i$$

$$x = \left(\frac{1}{2}\xi(1+\xi)\right)(L) + \left((1+\xi)(1-\xi)\right)\left(\frac{L}{4}\right) \quad (17)$$

$$= \frac{L}{4} + \frac{L}{2}\xi + \frac{L}{4}\xi^2$$

$$\xi = 2\sqrt{\frac{x}{L}} - 1 \quad .....(18)$$

Recalling that in isoparametric elements the displacement field along ($\eta = -1$) is given by equation (19).

Equation (19) can be re-written by replacing ξ with the previously derived expression, equation (18) it obtain equation (20). This complex equation can be rewritten in the form.

$$u = A + Bx + C\sqrt{\frac{x}{L}} \quad ..... (21)$$

It can be noted that the displacement field has had its quadratic term replaced by $x^{\frac{1}{2}}$, which means that when the derivative of the displacement is taken, the strain and stresses singularity order in ($\frac{1}{2}$).

Numerical results and discussion

A nonlinear finite element code is developed in MATLAB 8.0 using the present displacement field plate model in Green-Lagrange sense in the framework of the HSDT. The validation and accuracy of the present algorithm are examined by comparing the results with those available in the literature. The effect of different combinations of the thickness ratio (a/h), amplitude ratio (W_{max}/h), where W_{max} is the maximum deflection of plate and h is the thickness, and various oundary conditions on the composite plate response are also examined.

The following sets of boundary conditions are used for the present analysis'

a) Simply support boundary conditions (S):

$v = w = \phi_2 = \psi_2 = \theta_2 = 0$ at x=0,a

$u = w = \phi_1 = \psi_1 = \theta_1 = 0$ at y=0,b

b) Clamped boundary conditions (C)

$u = v = w = \phi_1 = \phi_2 = \psi_1 = \psi_2 = \theta_1 = \theta_2 = 0$ at x=0,a

$u = v = w = \phi_1 = \phi_2 = \psi_1 = \psi_2 = \theta_1 = \theta_2 = 0$ at y=0,b

A convergence of the mathematical model developed for laminated plate is presented. Figures (3) and (4) are shown the nondimensional fundamental frequency ($\varpi = \omega n_L \left(\frac{a^2}{h}\right)\sqrt{\left(\frac{\rho}{E_2}\right)}$), and frequency ratio $\left(\omega_{NL}/\omega_L\right)$ against mesh division respectively for simply support boundary condition and for different stacking sequences, The results are plotted using the material properties (*E₁=181 GPa, E₂=7.17GPa, G₂₃=6.71GPa, υ₁₂=0.28*, and the geometry parameters are *a/b=1, a/h=10*). From these figures it can be shown that the convergence is a (5X5) mesh, then it's used to compute the results throughout the study.

A comparison of the linear free vibration with out defect results with Classical Plate Theory (CPT) and the Layerwise plate theory (LWST) and the Generalized Lamination Plate Theory (GLPT) is also included. (GLPT, though identical in formulation with the Layerwise plate theory (LWST), does not consider the variation of the transverse displacement, w, through the thickness)(Samuel ,1992); and the results were obtained from a 3-D orthotropic elasticity theory (Noor,1975). The material properties and the geometries details of this comparison are:

$E_2 = E_3 = 1.0\times10^6\ psi$, $\frac{E_1}{E_2} = 3$, 10, 20, 30, $G_{12} = G_{13} = 0.6\times10^6\ psi$, $G_{23} = 0.5\times10^6\ psi$,

$\upsilon_{12} = \upsilon_{13} = 0.25$, $\upsilon_{23} = 0.24$,

$a = 20\ \ inch,\ \ b = 20\ \ inch,\ \ \frac{a}{h} = 10$.

The results are summarized in table (1). The differences are more pronounced between the present results and their results are existing in (Samuel ,1992 and Noor,1975), because the present work used in the framework of the high order shear theory and the other results used in the framework of the first order theory and classical theory.

When the plate containing some defect such as crack or hole, this causes decreasing in natural frequency with diverge in some results because the present work used in the framework of the high order shear theory and geometrical nonlinearity modeled using Green's strain. The results are shown in Table (2). The results of the linear fundamental frequency increase with increasing in modular ratio and decreasing in natural frequency in the damage case as shown in figure(4). The frequency ratio decreasing with increasing in modular ratio.

The variation of the frequency ratio for different support conditions and the amplitude ratios are analyzed for anti-symmetric and symmetric lamination schemes. The results are figured in table (3) . The effects of three different support conditions are examined on the frequency ratio such as all sides simple support (SSSS), all sides clamped (CCCC), and two sides simply support and two sides clamped (SCSC). The material properties and other parameters are ($E_1/E_2 = 15$, $G_{12}/E_2 = 0.5$, $G_{23}/E_2 = 0.2$, $\upsilon = 0.25$, $a/b = 1$, $a/h = 10$, and. It can be found that the fundamental frequency increased with increasing the amplitude ratio in all type of boundary condition and the frequency ratio for un-defect case are decreased when increasing amplitude ratio in some scheme but in another the frequency ratio are increased when increasing amplitude ratio laminated scheme because the effect of the high order shear theory.

The effect of damage size on the natural frequency, it is decreased the natural frequency with increasing the size of defect, because of the increased in the delamination size this lead to increase in reduction in stiffness matrix the results shown in table (4) and Figures (6).

The mode shape of the intact plate and crack plate are shown in the figures (7 & 8) which drawing by using the MATLAB Program. It can be noticed that the mode shape is decreased when the plate had contained the crack or hole.

Conclusions

The geometrically nonlinear free vibration analysis of composite plate with and without containing the crack or hole is investigated using nonlinear finite element method in the framework of a higher order shear deformation theory in Green-Lagrange sense. The governing equation of the vibrated plate is derived using the Variational approach. The frequency amplitude relations for the nonlinear free vibrated plate are computed using eigenvalue formulation and are solved employing a direct iterative procedure. Based on the numerical results the following conclusions are drawn.

1. The validation shows the necessities of taking into account full nonlinearity.
2. The two dimensional finite element model proposed can be predicted accurately the dynamic behaviors of a laminated composite plate with internal crack at arbitrary location.
3. The discrepancy of the results was (29.8249% when considered the severe nonlinearity).
4. Local internal crack has slight effect on the natural frequencies of the laminated composite plate although the extent of the natural frequency variation increased with both the damage dimension and the order of the natural frequency.
5. The frequency ratio is more pronounced when amplitude ratio increase.
6. The modular ratio and edge support condition affect the nonlinear frequencies.

References

[1]Adams R, D. et al, "Vibration Testing as a Non-Destructive Test Tool for Composite Materials" , Composite Reliability, ASTM STP580, pp. 159-175, 1975.

[2]Cawely P. & Adams R. D., "The Location of Defect in Structures Drom Measurements of Natural Frequencies", J. of Strain Analysis, Vol. 14, No. 2, pp. 49-57, 1979.

[3]James D. Lee, "Three Dimensional Finite Element Analysis of Damage Accumulation in Composite Laminate", Computers & Structures, Vol. 15, No. 3, pp. 335-350, 1982.

[4]Adam C. & Ziegler F, "Vibration of layered Beam Under Condition of Damaging and Slipping Interface", Int. J. Fracture, Vol.98, pp. 393, 1999.

[5]Yi Liu, Feng Jin and Qing Li, "A Strength – based Multiple Cutout Optimization in Composite plates Using Fixed Grid Finite Element Method", Composite Structures, Vol. (73), pp. (403-412), 2006.

[6]A.V. Singh and U.K. Paul, "Finite Displacement Static Analysis of Thin Plate With an Opening a Variational Approach", Int, J. of Solids & Structures, Vol. (40), pp.(4135-4151), 2003.

[7]Cengiz Polat & Zülfü Çinar ulucan, "Geometrically Non-Linear Analysis of Axisymmetric Plates and Shells", Int. J. of Science & Technolgy, Vol. 92, No.(1), pp.(33-40),2007.

[8]Noor, A.K., "Force Vibration of Multilayer Composite Plates", Vol. (11), pp. 1038-1051, 1975.

[9]Samuel Kinde Kassegne, "Layerwise Theory for Discretely Stiffened Laminated Cylindrical Shell", Virginia Polytechnic Institute and State University, Ph. D. , Thesis, December 1992.

[10]Fadhel Abbas Abdulla, "Effect of Internal Flaws in Dynamic Behavior of Composite Plate". Al-Mustansiriyah University, Engineering College, Thesis. October, 2005.

[11]Nabil Hassan Hadi and Kayser Aziz Ameen, "Nonlinear Free Vibration Of Cylindrical Shells With Delamination Using High Order Shear Deformation Theory :-A Finite Element Approach", American journal of Scientific and industrial Research, Vol. 2, Issue No. 2, pp. 251-277,2011.

Table (1) Nondimensional fundamental frequency of (0/90/0) and (0/90/0/90/0) cross-ply simply support plates

No. of layers	Method	E_{11}/E_{22}			
		3	10	20	30
3	LWST	0.2671	0.338	0.3897	0.4197
	GLPT	0.2645	0.3368	0.3897	0.4205
	3-D Elasticity	0.2647	0.3284	0.3824	0.4109
	CPT	0.2919	0.4126	0.5404	0.6433
	Present work	0.25699	0.343019	0.395955	0.4245764
5	LWST	0.2671	0.3429	0.4012	0.4354
	GLPT	0.2645	0.3415	0.4012	0.4367
	3-D Elasticity	0.2659	0.3409	0.3997	0.4314
	CPT	0.2919	0.4126	0.5404	0.6433
	Present work	0.332695	0.44010713	0.506355	0.5417735

Table (2) Effect of material orthotropy on nonlinear free vibration ratio $\left(\frac{\varpi_{NL}}{\varpi_L}\right)$ with crack length (a/3) in center of laminated plate

	W_{max}/h	E_1/E_2							
		3		5		10		15	
		κ_{cNL}	ϖ_{cNL}/ϖ_{cL}	κ_{cNL}	ϖ_{cNL}/ϖ_{cL}	κ_{cNL}	ϖ_{cNL}/ϖ_{cL}	κ_{cNL}	ϖ_{cNL}/ϖ_{cL}
0/90/0/90/0/90/0/90	0.5	0.057021039	1.863286914	0.180338035	1.637705543	0.033042735	1.938707427	0.142899684	1.836020005
	1	0.042025038	1.892714742	0.131596782	1.71476871	0.097010393	1.904191103	0.160028902	1.871903463
	1.5	0.051382177	1.992062358	0.113603155	1.770754418	0.142811394	1.86530864	0.148659887	1.880243416
	2	0.035671499	1.993707372	0.121160792	1.755655303	0.147143233	1.825947524	0.138411472	1.883651646
	ϖ_{cL}	56.44150326		70.44690689		67.60759767		71.79563929	
	κ_{cL}	0.11600686		0.034564061		0.090636347		0.034477866	
45/-45/45/-45/45/-45/45/-45	0.5	0.125709681	1.856340367	0.265264992	1.67255721	0.316079497	1.539095385	0.088375973	1.673798566

	1	0.116106973	1.87657956	0.181723224	1.9764999	0.289051354	1.807273715	0.149476372	1.699091253
	1.5	0.13884461	1.905126122	0.223872405	1.937803256	0.30049353	1.778187024	0.151558732	1.757734341
	2	0.138128233	1.906710814	0.197554247	2.003512626	0.295969643	1.846906095	0.202298398	1.73045089
	ϖ_{cL}	57.36175838		61.84191669		68.76180204		72.90931503	
	κ_{cL}	0.029015154		0.037515149		0.141159273		0.012513313	
0/45/-45/90/0/45/-45/90	0.5	0.705076975	1.853767436	0.142884767	1.814955527	0.09356096	1.817622008	0.13561697	1.737378006
	1	0.05756616	1.927861204	0.077081899	1.986220876	0.048816925	1.875118267	0.130827205	1.809828862
	1.5	0.073411178	1.993125546	0.102833381	1.992420725	0.160982018	1.821683444	0.18544703	1.784141009
	2	0.07657479	1.978725284	0.089984249	2.020954953	0.170875839	1.769633138	0.18689499	1.756860201
	ϖ_{cL}	56.47404261		60.80884518		67.67986643		71.87479574	
	κ_{cL}	0.082602942		0.091528083		0.089608847		0.033419227	

Table (3) Effect of material orthotropy on nonlinear free vibration ratio $\left(\frac{\varpi_{NL}}{\varpi_L}\right)$ with hole diameter (a/3) in center of laminated plate

Lay-up	W_{max}/h \ E_1/E_2	3		5		10		15	
		Kr_{hNL}	ϖ_{hNL}/ϖ_{hL}	Kr_{hNL}	ϖ_{hNL}/ϖ_{hL}	Kr_{hNL}	ϖ_{hNL}/ϖ_{hL}	Kr_{hNL}	ϖ_{hNL}/ϖ_{hL}
0/90/0/90/0/90/0/90	0.5	0.078000953	1.821831483	0.091799003	1.81460879	0.129128605	2.263853939	0.181284495	2.530439742
	1	0.084160311	1.809466165	0.029207622	1.916948668	0.094758951	2.308587206	0.120907558	2.497979688
	1.5	0.026150848	2.045047216	0.008928306	1.979863298	0.037730057	2.258180787	0.116674643	2.466253044
	2	0.022545807	2.020844171	0.035581434	2.068778929	0.036638121	2.219419349	0.125475195	2.460575013
	ϖ_{hL}	55.26664601		63.12624264		63.19763332		63.23289108	
	κ_{hL}	0.134407613		0.134889729		0.14995308		0.149631427	
45/-45/45/-45/45/-45/45/-45	0.5	0.140747443	1.824411378	0.082585642	2.088410082	0.155269286	1.900982846	0.006596989	2.251803771
	1	0.158439577	1.786703867	0.256378901	1.796173461	0.153371533	2.152179884	0.088744268	2.217982325
	1.5	0.05003775	2.101592718	0.138583123	2.150750005	0.124424076	2.225766042	0.095092255	2.284142765
	2	0.05060251	2.100343149	0.133014443	2.164652881	0.02809089	2.549641277	0.111816595	2.34751813
	ϖ_{hL}	52.61338292		53.71982456		56.26922209		57.23517444	
	κ_{hL}	0.109392756		0.098748313		0.066165478		0.055507033	
0/45/-45/90/0/45/-45/90	0.5	0.703568435	1.863249511	0.101338673	1.902930061	0.007977707	2.021230755	0.228962149	2.470168586
	1	0.000118682	2.045862452	0.210449717	1.699198719	0.12939994	2.226446742	0.118021959	2.327993261
	1.5	0.01153474	2.126223967	0.154278632	1.878171509	0.043341155	2.265311768	0.043781133	2.28622667
	2	0.012084516	2.116915722	0.156964827	1.872205076	0.084505453	2.31470373	0.039223699	2.245430463
	ϖ_{hL}	52.61338292		63.11303168		63.18935055		63.22422456	
	κ_{hL}	0.145317734		0.057104		0.150012718		0.149753134	

Table (4). Effect of variable boundary condition with crack defect (length a/3) in center of plate on the frequency ratio

	W_{max}/h	Boundary Condition					
		SSSS		SCSC		CCCC	
		Kr_{cNL}	ϖ_{cNL}/ϖ_{cL}	Kr_{cNL}	ϖ_{cNL}/ϖ_{cL}	Kr_{cNL}	ϖ_{cNL}/ϖ_{cL}
0/90/0/90/0/90/0/90	0.5	0.168846775	1.866372795	0.065789199	2.097790843	0.068795964	2.09133009
	1	0.152633343	1.895777346	0.06782112	2.085524122	0.070971741	2.07874335
	1.5	0.144434106	1.903672685	0.070054104	2.069171543	0.073443315	2.061872004
	2	0.137265086	1.906903723	0.072192663	2.050733356	0.075812243	2.042941548
	ϖ_{cL}	71.13562441		71.23251372		71.45227546	
	κ_{cL}	0.043587342		0.042372704		0.039192508	
45/-45/45/-45/45/-45/45/-45	0.5	0.07839721	1.684096732	0.124568504	1.965815104	0.110411613	1.997740722
	1	0.146107017	1.706215831	0.105523296	2.000679471	0.112855983	1.984423638
	1.5	0.142808911	1.765319098	0.108268685	1.982957707	0.115462988	1.967159127
	2	0.204096696	1.738129375	0.110871982	1.963267381	0.117855217	1.948144847
	ϖ_{cL}	72.22276044		72.46934732		73.07254351	
	κ_{cL}	0.027938465		0.025551366		0.01737698	
0/45/-45/90/0/45/-45/90	0.5	0.175055573	1.795321372	0.175055573	2.092695787	0.073076054	2.080965687
	1	0.197612951	1.793060518	0.197612951	2.079902749	0.075172596	2.068394548
	1.5	0.210356529	1.753099066	0.210356529	2.06295354	0.077491668	2.051661418
	2	0.2225075	1.712932491	0.2225075	2.043945232	0.079732142	2.032794887
	ϖ_{cL}	71.2173875		71.40275147	0.067911403	71.80892706	
	κ_{cL}	0.042427426		0.040093918		0.03471114	

Table (5). Effect of variable boundary condition with hole defect (diameter a/3 and in the center of plate) on the frequency ratio

	W_{max}/h	Boundary Condition					
		SSSS		SCSC		CCCC	
		Kr_{hNL}	$\varpi_{hNL}/\varpi_{hcL}$	Kr_{hNL}	$\varpi_{hNL}/\varpi_{hcL}$	Kr_{hNL}	$\varpi_{hNL}/\varpi_{hcL}$
0/90/0/90/0/90/0/90	0.5	0.181284495	2.530439742	0.053204623	2.028138571	0.059626535	2.109896804
	1	0.120907558	2.497979688	0.109635706	2.472859992	0.058399241	2.100183155
	1.5	0.116674643	2.466253044	0.0887141	2.404500255	0.068600721	2.363770455
	2	0.125475195	2.460575013	0.100056116	1.967506209	0.072919296	2.350698532
	ϖ_{hL}	63.23289108		63.2338454		63.23500388	
	κ_{hL}	0.149631427		0.149651532		0.149756717	
45/-45/45/-45/45/-45/45/-45	0.5	0.006596989	2.251803771	0.742228107	2.033535947	0.118678964	1.977478203
	1	0.088744268	2.217982325	0.091448154	2.025886137	0.066596941	2.378286871
	1.5	0.095092255	2.284142765	0.019517224	2.253384804	0.037726998	2.127118316

	2	0.111816595	2.34751813	0.075728237	2.353648347	0.076576396	2.356106505
	ϖ_{hL}	57.23517444		63.20741282		63.21093734	
	κ_{hL}	0.055507033		0.149891331		0.149930956	
0/45/-45/90/0/45/-45/90	0.5	0.228962149	2.470168586	0.095012082	2.030617115	0.061503643	2.381790085
	1	0.118021959	2.327993261	10442.17462	2.328830758	0.107073882	1.991440476
	1.5	0.043781133	2.28622667	0.119284509	2.474578926	0.062525301	2.349728248
	2	0.039223699	2.245430463	0.1119193	2.434007979	0.063884	2.329871254
	ϖ_{hL}	63.22422456		63.22443263		63.22652684	
	κ_{hL}	0.149753134		0.149766726		0.149780543	

Table (6). Effect of crack size on the frequency ratio

The position of crack in center of plate	Wmax/h	A(8)cm rc=WnNLC/WnLC	B(6)cm rc=WnNLC/WnLC	C(4)cm rc=WnNLC/WnLC
[0/90/0/90]s	0.5	1.930343359	4.086636398	1.921236218
	1	1.922313898	1.942084412	1.913323978
	1.5	1.911131566	1.931136304	1.902291511
	2	1.89803452	1.9182814	1.889360729
	ϖ_{cL}	76.88227081	76.87972951	75.71812343
[45/-45/45/-45]s	0.5	1.598392297	1.614759369	1.627163873
	1	1.605516333	1.66415144	1.611374134
	1.5	1.634458402	1.63654435	1.606963813
	2	1.615885563	1.607861998	1.616754759
	ϖ_{cL}	78.16249346	77.89880456	76.89350375
[0/45/-45/90]s	0.5	1.690942734	1.712428954	1.67699297
	1	1.681963842	1.698430168	1.665964374
	1.5	1.669615953	1.680274441	1.651226169
	2	1.65541835	1.665817514	1.634649585
	ϖ_{cL}	76.95194419	76.47627683	75.78892267

Table (7). Effect of hole size on the frequency ratio

The position of hole in center of plate	W_{max}/h	Hole Size					
		A(16 cm diameter)		A(13 cm diameter)		C(8 cm diameter)	
		κr_{hNL}	$\varpi_{hNL}/\varpi_{hcL}$	κr_{hNL}	$\varpi_{hNL}/\varpi_{hcL}$	κr_{hNL}	$\varpi_{hNL}/\varpi_{hcL}$
0/90/0/90/0/90/0/90	0.5	0.181284495	2.530439742	0.217868146	2.608805896	0.062993276	2.444468667
	1	0.120907558	2.497979688	0.158338905	2.581396685	0.127224773	2.252979077
	1.5	0.116674643	2.466253044	0.173252499	2.591209145	0.105462413	2.317933975
	2	0.125475195	2.460575013	0.173164597	2.564836176	0.09599095	2.318635114
	ϖ_{hL}	63.23289108		59.65697593		69.55419251	
	κ_{hL}	0.149631427		0.197721049		0.0646213	
45/-45/45/-45/45/-45/45/-45	0.5	0.226430983	2.251803771	0.073705509	1.971390277	0.999962967	6.79944E-05
	1	0.110267839	2.217982325	0.075933596	2.149392801	0.003314388	2.004321391
	1.5	0.102533494	2.284142765	0.205049489	2.496527395	0.095958614	2.270521442
	2	0.082156671	2.34751813	0.137374402	2.467301733	0.02942506	2.233127658
	ϖ_{hL}	57.23517444		59.63260199		67.0029219	
	κ_{hL}	0.224804502		0.192333647		0.092509739	
0/45/-45/90/0/45/-45/90	0.5	0.228962149	2.470168586	0.094871837	2.200652006	0.125328519	2.261868813
	1	0.118021959	2.327993261	0.220020781	2.54037958	0.010224782	2.060952398
	1.5	0.043781133	2.28622667	0.141146513	2.499489125	0.10273927	1.965298419
	2	0.039223699	2.245430463	0.141219639	2.465811107	0.026154854	2.217192861
	ϖ_{hL}	63.22422456		59.65375971		69.55416691	
	κ_{hL}	0.149753134		0.197769168		0.064627319	

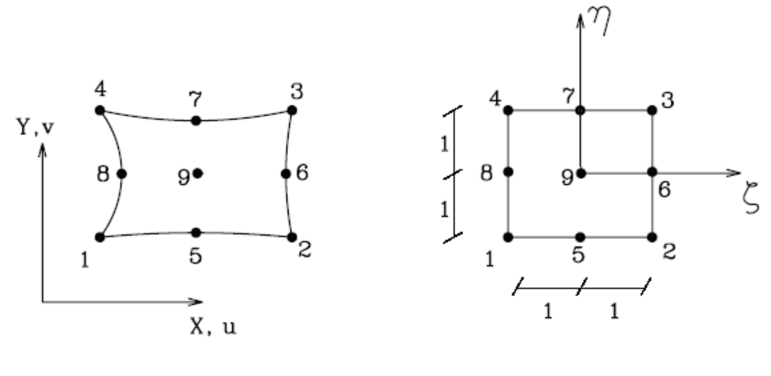

Figure (1) Rectangular Element

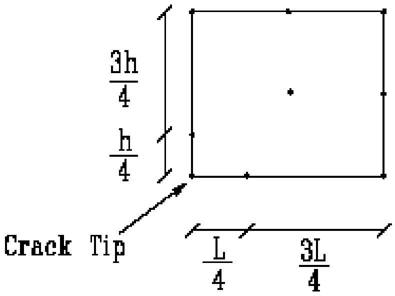

Figure (2) The element contain the crack tip

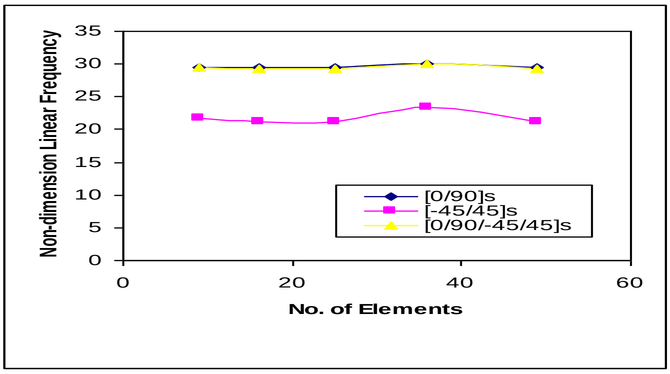

Figure (3). Convergence study of non-dimensional frequency for square plate having SSSS boundary condition with different stacking sequences

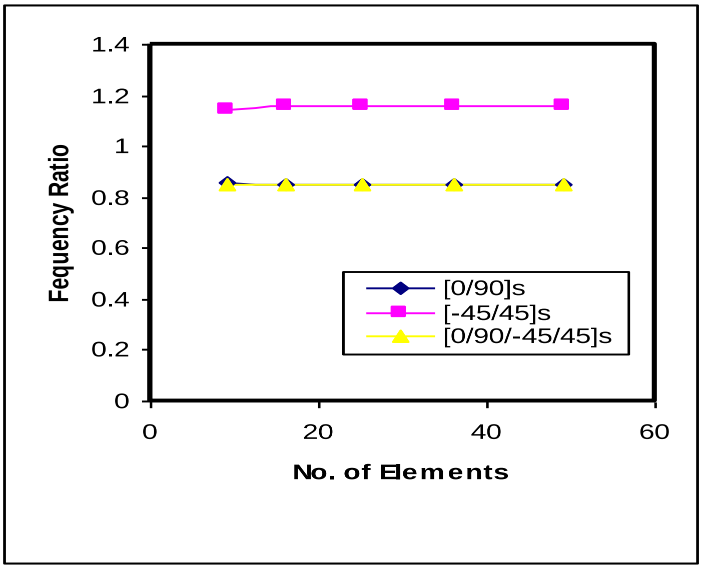

Figure (4). Convergence study for frequency ratio of square laminated plate with SSSS boundary condition with different stacking sequences

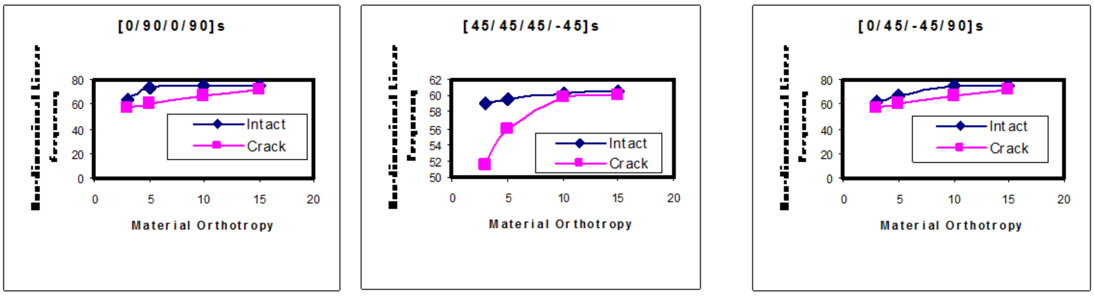

(A)

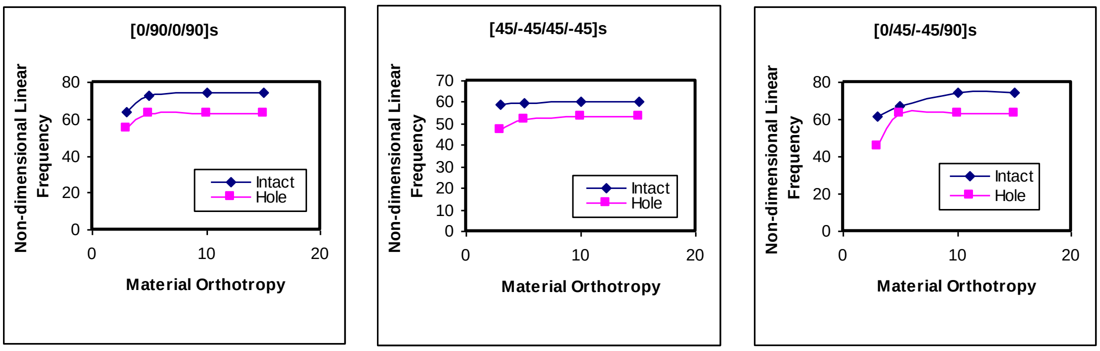

(B)

Figure (5). The linear fundamental frequency and material orthotropy for difference stacking sequence. (A) Crack damage, (B) Hole Damage.

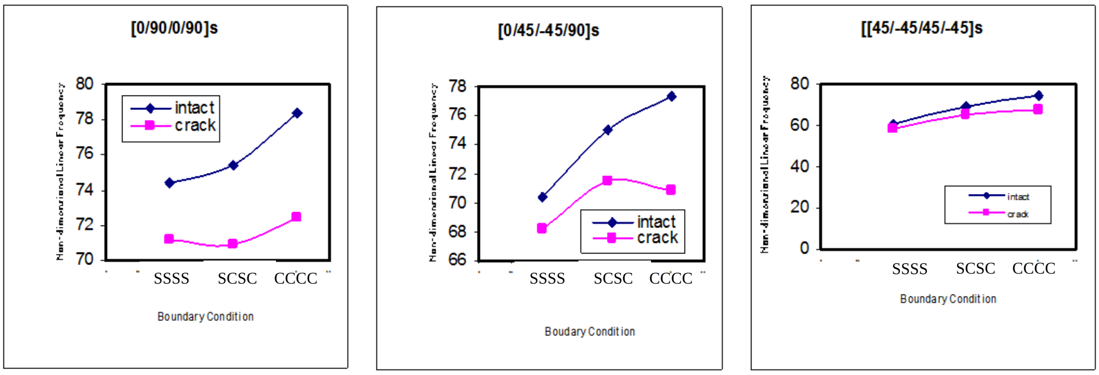

(A)

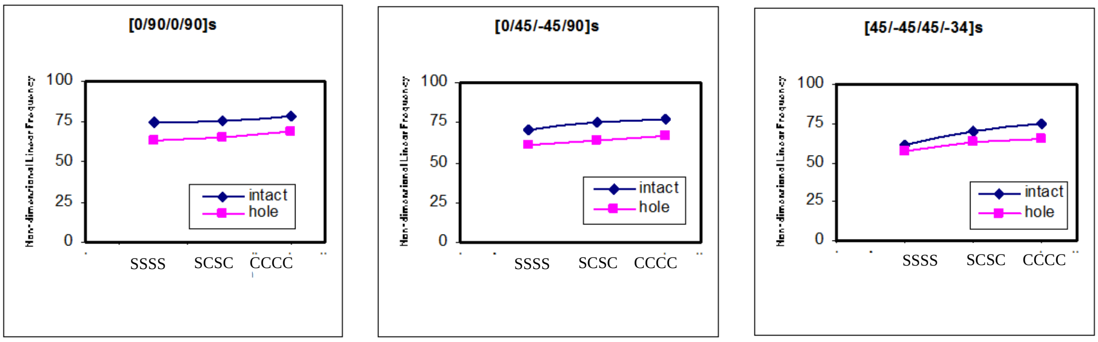

(B)

Figure (6). The linear fundamental frequency and boundary condition for difference stacking sequence. (A) Crack damage, (B) Hole damage.

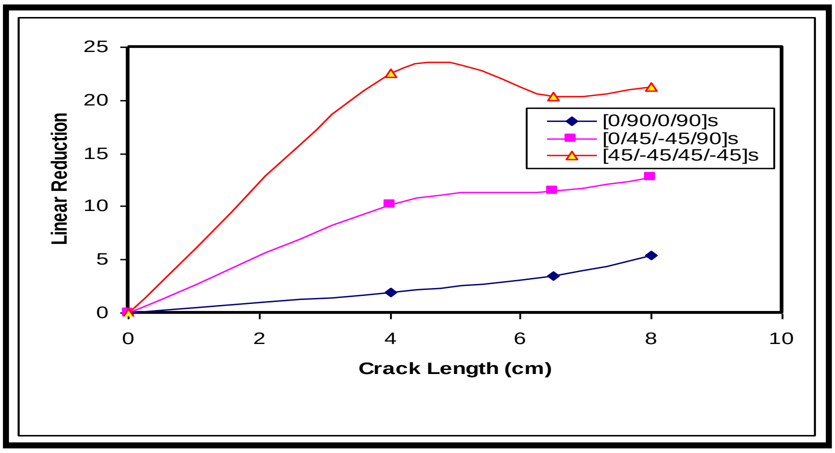

(A)

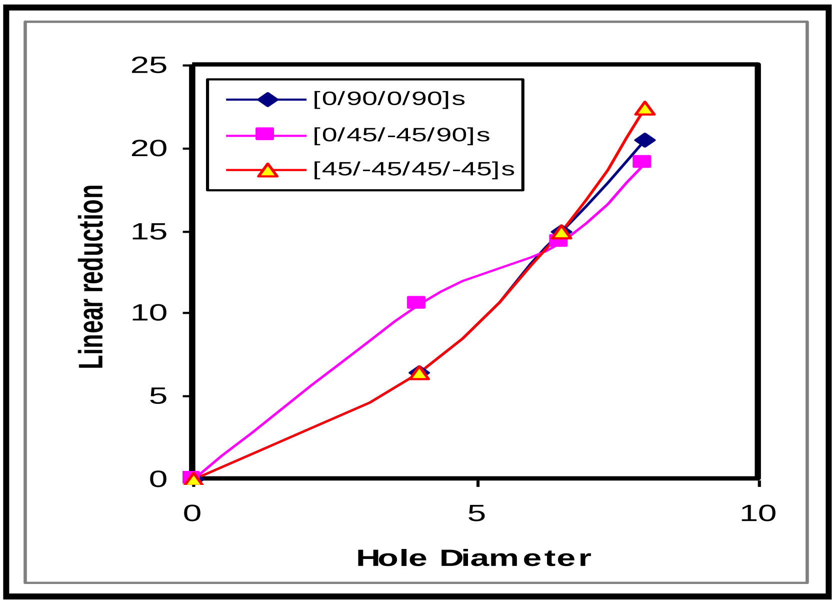

(B)

Figure (6). Reduction in natural frequency for intact and damage ((A)crack (B) hole) via. The size of damage

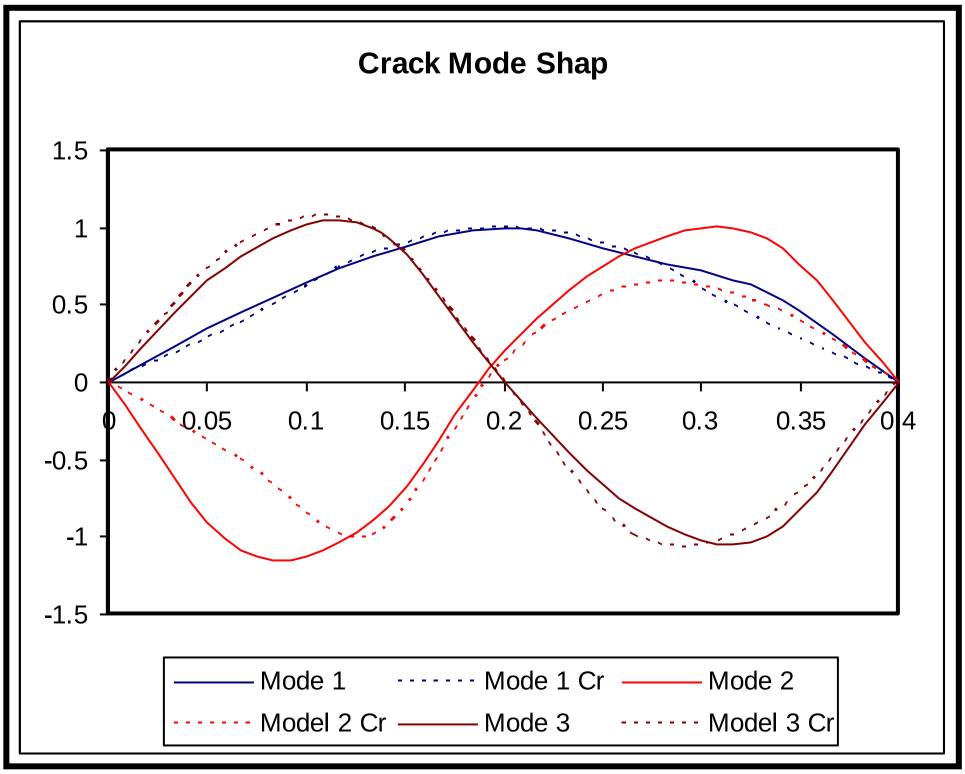

Figure (7). The mode shape of plate of the intact and crack plate [0/90/0/90]s

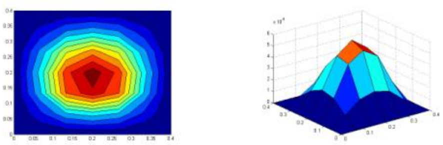

First Mode Shape

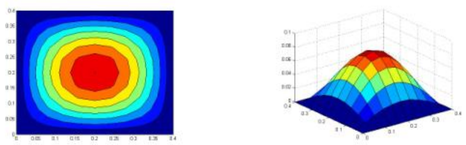

First Mode Shape

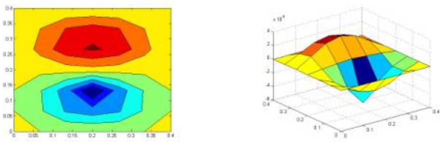

Second Mode Shape

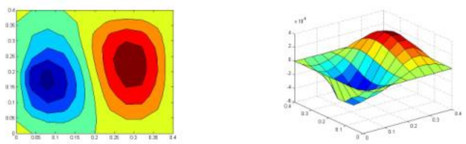

Second Mode Shape

Crack Plate Intact Plate

Figure (8). The surface and countour mode shape of plate of the intact and crack plate [0/90/0/90]s

Appendix (A)

$$\{\varepsilon\}=\begin{Bmatrix}\varepsilon_{\alpha,\alpha}\\ \varepsilon_{\beta,\beta}\\ \gamma_{\alpha,\beta}\\ \gamma_{\alpha,\zeta}\\ \gamma_{\beta,\zeta}\end{Bmatrix}=\begin{Bmatrix}\left(\dfrac{\partial \bar{u}}{\partial \alpha}\right)\\ \left(\dfrac{\partial \bar{v}}{\partial \beta}\right)\\ \left(\dfrac{\partial \bar{u}}{\partial \beta}+\dfrac{\partial \bar{v}}{\partial \alpha}\right)\\ \dfrac{\partial \bar{u}}{\partial \zeta}+\left(\dfrac{\partial \bar{w}}{\partial \alpha}\right)\\ \dfrac{\partial \bar{v}}{\partial \zeta}+\left(\dfrac{\partial \bar{w}}{\partial \beta}\right)\end{Bmatrix}+\frac{1}{2}\begin{Bmatrix}\left[\left(\dfrac{\partial \bar{u}}{\partial \alpha}\right)^2+\left(\dfrac{\partial \bar{v}}{\partial \alpha}\right)^2+\left(\dfrac{\partial \bar{w}}{\partial \alpha}\right)^2\right]\\ \left[\left(\dfrac{\partial \bar{v}}{\partial \beta}\right)^2+\left(\dfrac{\partial \bar{u}}{\partial \beta}\right)^2+\left(\dfrac{\partial \bar{w}}{\partial \beta}\right)^2\right]\\ 2\left[\left(\dfrac{\partial \bar{u}}{\partial \alpha}\right)\left(\dfrac{\partial \bar{u}}{\partial \beta}\right)+\left(\dfrac{\partial \bar{v}}{\partial \alpha}\right)\left(\dfrac{\partial \bar{v}}{\partial \beta}\right)+\left(\dfrac{\partial \bar{w}}{\partial \alpha}\right)\left(\dfrac{\partial \bar{w}}{\partial \beta}\right)\right]\\ 2\left[\left(\dfrac{\partial \bar{u}}{\partial \alpha}\right)\left(\dfrac{\partial \bar{u}}{\partial \zeta}\right)+\left(\dfrac{\partial \bar{v}}{\partial \alpha}\right)\left(\dfrac{\partial \bar{v}}{\partial \zeta}\right)+\left(\dfrac{\partial \bar{w}}{\partial \alpha}\right)\left(\dfrac{\partial \bar{w}}{\partial \zeta}\right)\right]\\ 2\left[\left(\dfrac{\partial \bar{v}}{\partial \beta}\right)\left(\dfrac{\partial \bar{v}}{\partial \zeta}\right)+\left(\dfrac{\partial \bar{u}}{\partial \alpha}\right)\left(\dfrac{\partial \bar{u}}{\partial \zeta}\right)+\left(\dfrac{\partial \bar{w}}{\partial \beta}\right)\left(\dfrac{\partial \bar{w}}{\partial \zeta}\right)\right]\end{Bmatrix}$$

Or, $\{\varepsilon\}=\{\varepsilon_L\}+\{\varepsilon_{NL}\}$ (2)

Where $\{\varepsilon_L\}$ and $\{\varepsilon_{NL}\}$ are the linear and nonlinear strain vectors respectively.

$$\{\varepsilon_L\}+\{\varepsilon_{NL}\}=\begin{Bmatrix}\varepsilon_1^0\\ \varepsilon_2^0\\ \varepsilon_6^0\\ \varepsilon_5^0\\ \varepsilon_4^0\end{Bmatrix}+\frac{1}{2}\begin{Bmatrix}\varepsilon_1^4\\ \varepsilon_2^4\\ 2\varepsilon_6^4\\ 2\varepsilon_5^4\\ 2\varepsilon_4^4\end{Bmatrix}+\zeta\left[\begin{Bmatrix}\chi_1^1\\ \chi_2^1\\ \chi_6^1\\ \chi_5^1\\ \chi_4^1\end{Bmatrix}+\frac{1}{2}\begin{Bmatrix}\chi_1^5\\ \chi_2^5\\ 2\chi_6^5\\ 2\chi_5^5\\ 2\chi_4^5\end{Bmatrix}\right]+\zeta^2\left[\begin{Bmatrix}\chi_1^2\\ \chi_2^2\\ \chi_6^2\\ \chi_5^2\\ \chi_4^2\end{Bmatrix}+\frac{1}{2}\begin{Bmatrix}\chi_1^6\\ \chi_2^6\\ 2\chi_6^6\\ 2\chi_5^6\\ 2\chi_4^6\end{Bmatrix}\right]$$

$$+\zeta^3\left[\begin{Bmatrix}\chi_1^3\\ \chi_2^3\\ \chi_6^3\\ \chi_5^3\\ \chi_4^3\end{Bmatrix}+\frac{1}{2}\begin{Bmatrix}\chi_1^7\\ \chi_2^7\\ 2\chi_6^7\\ 2\chi_5^7\\ 2\chi_4^7\end{Bmatrix}\right]+\zeta^4\left[\frac{1}{2}\begin{Bmatrix}\chi_1^8\\ \chi_2^8\\ 2\chi_6^8\\ 2\chi_5^8\\ 2\chi_4^8\end{Bmatrix}\right]+\zeta^5\left[\frac{1}{2}\begin{Bmatrix}\chi_1^9\\ \chi_2^9\\ 2\chi_6^9\\ 2\chi_5^9\\ 2\chi_4^9\end{Bmatrix}\right]+\zeta^6\left[\frac{1}{2}\begin{Bmatrix}\chi_1^{10}\\ \chi_2^{10}\\ 2\chi_6^{10}\\ 0\\ 0\end{Bmatrix}\right] \quad (3)$$

$$\{\varepsilon\}=\{\varepsilon_L\}+\{\varepsilon_{NL}\}=[\Im]_L\{\overline{\varepsilon}\}_L+\frac{1}{2}[\Im]_{NL}\{\overline{\varepsilon}\}_{NL} \quad (4)$$

Where

$$\{\overline{\varepsilon}\}_L=\{\varepsilon_1^0\ \ \varepsilon_2^0\ \ \varepsilon_6^0\ \ \varepsilon_5^0\ \ \varepsilon_4^0\ \ \chi_1^1\ \ \chi_2^1\ \ \chi_6^1\ \ \chi_5^1\ \ \chi_4^1\ \ \chi_1^2\ \ \chi_2^2\ \ \chi_6^2\ \ \chi_5^2\ \ \chi_4^2\ \ \chi_1^3\ \ \chi_2^3\ \ \chi_6^3\ \ \chi_5^3\ \ \chi_4^3\}$$

$$\{\overline{\varepsilon}\}_{NL}=\{\varepsilon_1^4\ \ \varepsilon_2^4\ \ \varepsilon_6^4\ \ \varepsilon_5^4\ \ \varepsilon_4^4\ \ \chi_1^5\ \ \chi_2^5\ \ \chi_6^5\ \ \chi_5^5\ \ \chi_4^5\ \ \chi_1^6\ \ \chi_2^6\ \ \chi_6^6\ \ \chi_5^6\ \ \chi_4^6\ \ \chi_1^7\ \ \chi_2^7\ \ \chi_6^7\ \ \chi_5^7\ \ \chi_4^7\ \ \chi_1^8\ \ \chi_2^8\ \ \chi_6^8\ \ \chi_5^8\ \ \chi_4^8\ \ \chi_1^9\ \ \chi_2^9\ \ \chi_6^9\ \ \chi_5^9\ \ \chi_4^9\ \ \chi_1^{10}\ \ \chi_2^{10}\ \ \chi_6^{10}\}$$

$$\begin{Bmatrix}\sigma_\alpha\\ \sigma_\beta\\ \sigma_{\alpha\beta}\\ \sigma_{\alpha\zeta}\\ \sigma_{\beta\zeta}\end{Bmatrix}^k=\begin{bmatrix}\overline{Q}_{11} & \overline{Q}_{12} & \overline{Q}_{16} & 0 & 0\\ \overline{Q}_{12} & \overline{Q}_{22} & \overline{Q}_{26} & 0 & 0\\ \overline{Q}_{16} & \overline{Q}_{26} & \overline{Q}_{66} & 0 & 0\\ 0 & 0 & 0 & \overline{Q}_{55} & \overline{Q}_{45}\\ 0 & 0 & 0 & \overline{Q}_{45} & \overline{Q}_{44}\end{bmatrix}^k\left[\begin{Bmatrix}\varepsilon_1\\ \varepsilon_2\\ \varepsilon_6\\ \varepsilon_5\\ \varepsilon_4\end{Bmatrix}^k\right] \quad (5)$$

Where :

$$\overline{Q}_{11}=Q_{11}\cdot\cos^4\vartheta+2(Q_{12}+2Q_{66})\cdot\sin^2\vartheta\cdot\cos^2\vartheta+Q_{22}\cdot\sin^4\vartheta$$

$$\overline{Q}_{12} = (Q_{11} + Q_{22} - 4Q_{66}) \cdot \sin^2\vartheta \cdot \cos^2\vartheta + Q_{11}(\cos^4\theta + \sin^4\vartheta)$$
$$\overline{Q}_{22} = Q_{11}\sin^4\vartheta + 2(Q_{12} + 2Q_{66})\sin^2\vartheta \cdot \cos^2\vartheta + Q_{22}\cos^4\vartheta$$
$$\overline{Q}_{16} = (Q_{11} - Q_{12} - 2Q_{66})\sin\vartheta \cdot \cos^3\vartheta + (Q_{12} - Q_{22} + 2Q_{66})\sin^3\vartheta \cdot \cos\vartheta$$
$$\overline{Q}_{26} = (Q_{11} - Q_{12} - 2Q_{66})\sin^3\vartheta \cdot \cos\vartheta + (Q_{12} - Q_{22} + 2Q_{66})\sin\vartheta \cdot \cos^3\vartheta$$
$$\overline{Q}_{66} = (Q_{11} + Q_{22} - 2Q_{12} - 2Q_{66})\sin^2\vartheta \cdot \cos^2\vartheta + Q_{66}(\sin^4\vartheta + \cos^4\vartheta)$$
$$\overline{Q}_{44} = Q_{44}\cos^2\vartheta + Q_{55}\sin^2\vartheta$$
$$\overline{Q}_{45} = (Q_{55} - Q_{44})\cos\vartheta \cdot \sin\vartheta$$
$$\overline{Q}_{55} = Q_{55}\cos_2\vartheta + Q_{44}\sin_2\vartheta$$

$$U = \frac{1}{2}\int_V \{\varepsilon_L + \varepsilon_{NL}\}_i^T \left[\overline{Q}\right]\{\varepsilon_L + \varepsilon_{NL}\}_i \, dV$$

$$= \frac{1}{2}\int\left(\{\varepsilon_L\}_i^T [D_1]\{\varepsilon_L\}_i + \frac{1}{2}\{\varepsilon_L\}_i^T [D_2]\{\varepsilon_{NL}\}_i + \frac{1}{2}\{\varepsilon_{NL}\}_i^T [D_3]\{\varepsilon_L\}_i + \frac{1}{4}\{\varepsilon_{NL}\}_i^T [D_4]\{\varepsilon_{NL}\}_i \right) dA \quad (7)$$

Where :

$$[D_1] = \sum_{k=1}^{N} \int_{\zeta_{k-1}}^{\zeta_k} [\Im]_L^T \left[\overline{Q}\right] [\Im]_L \, d\zeta$$
$$[D_2] = \sum_{k=1}^{N} \int_{\zeta_{k-1}}^{\zeta_k} [\Im]_L^T \left[\overline{Q}\right] [\Im]_{NL} \, d\zeta$$
$$[D_3] = \sum_{k=1}^{N} \int_{\zeta_{k-1}}^{\zeta_k} [\Im]_{NL}^T \left[\overline{Q}\right] [\Im]_L \, d\zeta$$
$$[D_4] = \sum_{k=1}^{N} \int_{\zeta_{k-1}}^{\zeta_k} [\Im]_{NL}^T \left[\overline{Q}\right] [\Im]_{NL} \, d\zeta$$

Where : N is the numbers of layers

$$\left\{\dot{\bar{\delta}}\right\}_i = \begin{Bmatrix} \dot{\bar{u}} \\ \dot{\bar{v}} \\ \dot{\bar{w}} \end{Bmatrix} = \begin{bmatrix} 1 & 0 & 0 & \zeta & 0 & \zeta^2 & 0 & \zeta^3 & 0 \\ 0 & 1 & 0 & 0 & \zeta & 0 & \zeta^2 & 0 & \zeta^3 \\ 0 & 0 & 1 & 0 & 0 & 0 & 0 & 0 & 0 \end{bmatrix} \begin{Bmatrix} \dot{u} \\ \dot{v} \\ \dot{w} \\ \dot{\phi}_1 \\ \dot{\phi}_2 \\ \dot{\psi}_1 \\ \dot{\psi}_2 \\ \dot{\theta}_1 \\ \dot{\theta}_2 \end{Bmatrix} = [f]\{\dot{\delta}\} \qquad (9)$$

Where, [f] is the function of the thickness coordinate.

$$U = \frac{1}{2}\int_A \Bigg([B_L]_i^T \{\delta\}_i^T [D_1][B_L]_i \{\delta\}_i + \frac{1}{2}[B_L]_i^T \{\delta\}_i^T [D_2][B_{NL}]_i \{\delta\}_i + \frac{1}{2}[B_{NL}]_i^T \{\delta\}_i^T [D_3][B_L]_i \{\delta\}_i$$
$$\frac{1}{4}[B_{NL}]_i^T \{\delta\}_i^T [D_4][B_{NL}]\{\delta\}_i^T \Bigg) dA \qquad (12)$$

Where $[B_{NL}]_i = [A]_i [G]_i$, $[A]_{33\times27}$ is function to the displacements and $[G]_{27\times9}$ is the product form of differential operator and shape function in the nonlinear strain terms. $[B_L]_{20\times9}$ is the product form of the differential operator and nodal interpolation function in the linear terms.

$$\left.\frac{\partial x}{\partial \xi}\right|_{\eta=-1} = \left(\frac{1}{2}\xi + + \frac{1}{2}(\xi-1)\right)(0) + \left(\frac{1}{2}\xi + \frac{1}{2}(\xi+1)\right)(L) + \left(-1\times\xi\times(-1+1)\times\frac{1}{4} - \frac{1(-1+1)(\xi+1)}{4}\right)(L)$$
$$\left(-\xi(-1+1)\frac{1}{4} + -1(-1+1)(\xi-1)\frac{1}{4}\right)(0) + \left(\frac{-1\times(-1-1)(\xi-1)}{2} - \frac{(-1\times(-1-1)(\xi+1))}{2}\right)x_5$$
$$+\left(\frac{(-\xi(-1-1)(-1+1))}{2} - \frac{(-1-1)(-1+1)(\xi+1)}{2}\right)(L) + \left(\frac{(-1+1)(\xi-1)}{2} - \frac{(-(-1+1)(\xi+1))}{2}\right)\left(\frac{L}{2}\right)$$
$$+\left(\frac{-(\xi(-1-1)(-1+1))}{2} - \frac{((-1-1)(-1+1)(\xi-1))}{2}\right)(0)$$
$$+((-1-1)(-1+1)(\xi-1) + (-1-1)(-1+1)(\xi+1))\left(\frac{L}{2}\right) \qquad (16)$$

$$u = u_1\left[\frac{1}{2}\xi(\xi-1)\right] + u_5\left[(1+\xi)(1-\xi)\right] + u_2\left[\frac{1}{2}\xi(1+\xi)\right] \quad (19)$$

$$u = u_1\left[\left(2\sqrt{\frac{x}{L}}-1\right)\left(1+\sqrt{\frac{x}{L}}\right)\right] + u_5\left[4\sqrt{\frac{x}{L}}\left(1-\sqrt{\frac{x}{L}}\right)\right] + u_2\left[\sqrt{\frac{x}{L}}\left(2\sqrt{\frac{x}{L}}-1\right)\right] \quad (20)$$